Controllable electric field tuning of anisotropic magnetic response of Ni/PMN-PT heterostructures

Yuanzhi Xiang¹, Peng Zhou^{1,†}, Kun Liang^{1,‡}, Yajun Qi¹, Zhijun Ma¹, Ying Liu^{1,2}, Zhuo Yan¹, Pengcheng Du¹, Rui Xiong³, Yong Liu³, Zhengcai Xia⁴, Maksym Popov^{2,5}, Dmitry Filippov⁶, Jitao Zhang⁷, Gopalan Srinivasan², and Tianjin Zhang^{1,*}

¹Hubei Collaborative Innovation Center for Advanced Organic Chemical Materials, Key Laboratory of Green Preparation and Application for Materials, Ministry of Education, Hubei Provincial Key Laboratory of Polymers, Department of Materials Science and Engineering, Hubei University, Wuhan 430062, China

²Physics Department, Oakland University, Rochester, Michigan 48309, USA

³School of Physics and Technology, and the Key Laboratory of Artificial Micro/Nano Structures of Ministry of Education, Wuhan University, Wuhan 430072, China

⁴Wuhan National High Magnetic Field Center & School of Physics, Huazhong University of Science and Technology, Wuhan 430074, China

⁵Faculty of Radiophysics, Electronics and Computer Systems, Taras Shevchenko National University of Kyiv, Kyiv 01601, Ukraine

⁶Novgorod State University, Veliky Novgorod 173003, Russia

⁷College of Electrical and Information Engineering, Zhengzhou University of Light Industry, Zhengzhou 450002, China

†p zhou@outlook.com (Peng Zhou)

‡<u>liangkun@hubu.edu.cn</u> (Kun Liang)

*zhangtj@hubu.edu.cn (Tianjin Zhang)

Abstract

Epitaxial Ni films with various thicknesses were grown on (001)-oriented 0.7Pb(Mg_{1/3}Nb_{2/3})O₃-

0.3PbTiO₃ (PMN-PT) substrates. Electric field tuning (E-tuning) of ferromagnetic resonance field

 (H_r) was utilized to investigate the magnetic response of Ni films along different film directions.

Butterfly-like H_r vs E curves are shown when magnetic field is applied along film edge. While the

combination of both loop-like and butterfly-like $H_{\rm r}$ vs E curves are observed for Ni film with

thicknesses of 180 nm and 240 nm, and merely loop-like curves can be seen for film thicknesses

of 330 nm and 510 nm, as magnetic field is applied along film diagonal. These interesting

phenomena are assumed to be related to ferroelectric and ferroelastic domain switching in

PMN-PT, film strain status, as well as magnetic anisotropy in Ni film. This work demonstrates the

feasibility of control of anisotropic magnetic response via electric field in multiferroic

heterostructure.

Keywords: electric field tuning, ferromagnetic resonance field, magnetic response, anisotropy

2

Introduction

The manipulation of magnetic properties by an electric field in magnetoelectric (ME) multiferroic materials has driven significant research activity due to its transformative technological potential in the field of electric-field control of magnetism, radio- and high-frequency devices, ultralow power logic-memory devices, and so on^[1, 2]. ME composite consists of ferromagnetic (FM) thin film and piezoelectric substrate with high electromechanical coupling coefficient is of great significance for achieving high ME coupling coefficient ^[3-5]. 0.7Pb(Mg_{1/3}Nb_{2/3})O₃–0.3PbTiO₃ (PMN–PT) single crystal is one of the most popular piezoelectric substrates that has been utilized in ME composites. It has ultrahigh piezoelectric response, large electric field strain values, and the composition of which is near the morphotropic phase boundary (MPB) ^[6-8]. Yang *et al.* demonstrated an approach to realize non-volatile strain in (001)-oriented PMN-PT single crystal, *i.e.*, loop-like strain-electric field (*S-E*) curves was shown under pulsed electric field, which is related to the 109° ferroelastic domain switching ^[9]. In most cases, the strain induced by converse piezoelectric effect is volatile and the involved *S-E* curve is butterfly-like ^[10].

We have seen the great achievement in both obtaining high ME response and exploring the potential mechanisms in terms of FM thin film/PMN-PT composites (FM/PMN-PT). In general, electric-field tuning (*E*-tuning) of magnetization and ferromagnetic resonance (FMR) field are two of the commonly used methods for study of converse ME effect. Based on the composite of Co₄₀Fe₄₀B₂₀(CoFeB)/PMN-PT (001), three types of magnetic responses induced by different types of ferroelectric domain switching in PMN-PT were spatially resolved via magneto-optic Kerr effect and scanning electron microscopy with polarization analysis with in situ electric fields [11]. The 90° rotation of magnetic easy axis was controlled by 109° ferroelastic domain switching. Similarly, Li *et al.* revealed the coexistence of loop-like (non-volatile) and butterfly-like (volatile) magnetic behaviors in CoFeB/PMN-PT (001) heterostructure, which is because of the 109° and the 71°/180° domain switching, respectively^[12]. In 2012, Zhang *et al.* investigated the electric-field control of nonvolatile magnetization in the same heterostructure, which is related to the combined action of 109° ferroelastic domain switching and the absence of magnetocrystalline anisotropy in CoFeB [13]. Using similar research methods, some other FM/PMN-PT composites

were also considered recently, *i.e.*, Co/PMN-PT^[14, 15], γ' -Fe₄N/PMN-PT ^[16], Co₂FeAl/PMN-PT ^[17], LiFe₅O₈/PMN-PT ^[18], Fe/PMN-PT ^[19, 20], Fe₃O₄/PMN-PT ^[21], Ni_{0.5}Zn_{0.5}Fe₂O₄/PMN-PT ^[22], La_xSr_{1-x}MnO₃/PMN-PT ^[23, 24].

There are basically three possible mechanisms that dominate in E-tuning of magnetic properties in FM/PMN-PT heterostructures. The first one is strain (interfacial strain) control of magnetism, the second one is charge-mediated magnetism, and the last one is magnon-driven ME coupling. Strain-mediated ME coupling is usually for thick FM films (more than 100 nm), while charge-screening at the FM surface is pronounced on the scale of a few angstroms [25]. Magnon-driven ME coupling, however, is dominant over tens of nanometers for FM layers [19]. For E-tuning of FMR, resonance field vs electric field (H_r vs E) shows butterfly-like curve because of strain-mediated effect and loop-like curve for the reason of charge-screening or magnon-driven effects. On the other hand, the loop-like and butterfly-like H_r vs E curves can also be induced by 109° ferroelastic and 71/180° ferroelectric domain switching, respectively.

So far the phenomena about loop-like and butterfly-like H_r vs E curves or magnetization vs electric field curves that are shown in FM/PMN-PT heterostructures have been intensively studied. Only one of the loop-like and butterfly-like curves was usually observed in individual work [13, 16-19, 26]. By inserting a nonmagnetic layer between FM layer and PMN-PT, we could also see both curves in the samples with and without that inserted layer [14, 27]. Interestingly, both curves could be shown at various ferroelastic/ferroelectric domains in an individual sample via microscopic characterization methods (magneto-optic Kerr effect) [11]. Or one curve could be deduced from the other one [12]. Zhu *et al.* reported the observation of both loop-like and butterfly-like resistance vs electric field curves at different temperatures, which is resulted from coaction and competition between the ferroelectric field effect and the strain effect in $Pr_{0.5}Ca_{0.5}MnO_3/PMN-PT$ [28]. To the best of our knowledge, there is only one study shows both loop-like and butterfly-like magnetization vs electric field curves in an individual sample at different directions at room temperature, where the composition of PMN-0.18PT is far from MPB region [29].

In this work, epitaxial nickel (Ni) films with thicknesses of 180 nm, 240 nm, 330 nm, and 510 nm

were deposited on (001)-oriented PMN-PT single crystal substrates. Electric field control of in-plane FMR field with magnetic field applied along edge (0°) and diagonal (45°) (see figure S1 in supplementary information) was investigated in detail. Only butterfly-like H_r vs E curves are shown when magnetic field is applied along film edge. While the combination of both loop-like and butterfly-like H_r vs E curves are observed for Ni film with thicknesses of 180 nm and 240 nm, and merely loop-like curves can be seen for film with thicknesses of 330 nm and 510 nm, as magnetic field is applied along diagonal. These interesting phenomena are assumed to be correlated with ferroelectric and ferroelastic domain switching in PMN-PT, film strain status, as well as magnetic anisotropy in Ni film. The present work is of significance for further understanding of electric field control of converse ME effect in FM/PMN-PT heterostructures.

Experiment

Ni films with thicknesses of 180 nm, 240 nm, 330 nm, and 510 nm were grown on commercially obtained (001)-oriented PMN-PT single crystal substrates by magnetron sputtering with Ar pressure and deposition power of 0.5 Pa and 50 W, respectively, at growth temperature of 500 °C. All of the films were in-situ annealed at 500 °C for 1 h. Subsequently, 40 nm Pt layers were deposited on top of Ni film and the other side of PMN-PT, which were used as electrodes for applying electric field and capping layer for preventing oxidation.

The structural properties were measured by X-ray diffraction (XRD) using a Bruker D8 Discover four-circle diffraction system ($CuK_{\alpha l}$, $\lambda = 1.5406$ Å). Dynamic magnetic properties were characterized via FMR (Bruker, EMX Plus), and magnetic force microscope (MFM) and piezoelectric force microscope (PFM) (Asylum Research MFP-3D Origin). All of the measurements were conducted at room temperature.

Results and discussion

Figures 1(a) and (b) show XRD θ -2 θ and ϕ -scan of (001)-oriented Ni/PMN-PT heterostructure, where Ni is 180 nm. Only (002) diffraction peak is detected in figure 1(a). The film and substrate show diffraction peaks at the same values of ϕ , in which they both have four-fold symmetry,

indicating epitaxial growth of Ni film, see figure 1(b). The epitaxial relationship between film and substrate can be written as: Ni (001)[010] || PMN-PT (001)[010]. Similar analyses for other (001)-oriented Ni/PMN-PT heterostructures with Ni thicknesses of 240 nm, 330 nm, and 510 nm, were also conducted, please refer to our previous work [30].

Static MFM image for as-grown 180 nm thick Ni film shows magnetic stripe domain, see figure 1(c). In MFM, magnetic probe detects only the magnetic dipole with magnetization perpendicular to the sample surface [31], which means the film has partial magnetic moment perpendicular to the film surface.

Figure 2 illustrates angular dependent H_r of as-grown Ni films. The experimental data were fitted based on the following formula [32, 33]:

$$f = \gamma \sqrt{(H_r + 4\pi M_{eff} + (\frac{3}{4} + \frac{1}{4}\cos(4\theta))H_4)(H_r + H_4\cos(4\theta))}$$
(1)

Where resonance frequency f is fixed to 9.85 GHz in this work, γ is gyromagnetic ratio with value of 3.05 GHz/kOe ^[34], H_r and H_4 are resonance field and cubic magnetocrystalline anisotropy field, respectively, θ is the angle between in-plane magnetic field and the sample edge, and $M_{\rm eff}$ is effective magnetization. Magnetic easy axes and hard axes lie in diagonal and edge, respectively. 510-nm-thick film shows standard four-fold symmetry, while the films with other thicknesses obviously deviate from four-fold symmetry at 0° and 180°, see figures 2(a) and S2. This deviation is believed related to the structure of PMN-PT substrate. Since PMN-PT utilized here has complicated phase structures ^[13, 35, 36], it's not absolute four-fold symmetric structure, as seen the peak-split in figure 1(a). On the other hand, for magnetic properties of Ni films, the contributions from strained and relaxed Ni films are different. The influence of strained Ni film (close to film and substrate interface) on magnetic or E-tuning magnetic properties should be considered until the Ni film is thick enough, where the strained Ni film is part of the whole Ni film for individual sample. Strained part of Ni films with thickness of 180 nm, 240 nm, and 330 nm may still play an important role in the relative magnetic and E-tuning of magnetic response. Detailed discussions please refer to Supplementary information. According to formula (1), we calculated the values of

 $M_{\rm eff}$ and H_4 , as well as magnetoelastic anisotropy field ($H_m = 4\pi M_{eff} - H_4$, see supplementary information for details) for each film, as listed in Table I. $M_{\rm eff}$ and absolute values of H_4 decrease as the increase of film thickness. The lowest and highest $H_{\rm m}$ appears in 510 nm thick and 180 nm thick Ni films, respectively, with the $H_{\rm m}$ difference of more than 1.3 kOe.

Dynamic magnetic properties were characterized by in-plane FMR under electric field along different directions. The relationship between H_r and E as well as H_{me} and E at 0° and 45° is shown in figures 3 and 4 for samples with thicknesses of 180 nm and 510 nm, respectively, where the electric field is scanned from 0 to 10 kV/cm, then to -10 kV/cm, and finally goes back to 0. H_{me} is the E-induced anisotropy field, which is determined by the following formula:

$$f = \gamma \sqrt{(H_r + 4\pi M_{eff} + (\frac{3}{4} + \frac{1}{4}\cos(4\theta))H_4 + H_{me})(H_r + H_4\cos(4\theta) + H_{me})}$$
(2)

For $\theta = 0^{\circ}$,

$$f = \gamma \sqrt{(H_r + 4\pi M_{eff} + H_4 + H_{me})(H_r + H_4 + H_{me})}$$
(3)

For $\theta = 45^{\circ}$,

$$f = \gamma \sqrt{(H_r + 4\pi M_{eff} + 0.5H_4 + H_{me})(H_r - H_4 + H_{me})}$$
(4)

Then $H_{\rm me}$ can be calculated using formulas (3) and (4). When magnetic field is applied along edge, both $H_{\rm r}$ vs E and $H_{\rm me}$ vs E show butterfly-like behavior for these two samples. Interestingly, $H_{\rm r}$ vs E and $H_{\rm me}$ vs E illustrate combination of butterfly-like and loop-like behavior for the sample with Ni film thickness of 180 nm, while there is only loop-like behavior shown for the sample with 510 nm thick Ni film, as magnetic field is applied along diagonal. In fact, the combination of butterfly-like and loop-like behavior exist in samples with Ni film thicknesses of 180 nm and 240 nm, nevertheless only loop-like behavior is observed for 330 nm and 510 nm thick Ni films, when magnetic field is applied along diagonal, see figures S3 and S4. Merely butterfly-like behavior can be seen as magnetic field is applied along edge for all of the samples. The largest E-tuning $H_{\rm r}$ shift is about 630 Oe, which occurs as magnetic field applied along edge for Ni film with thickness of 240 nm, corresponding to the converse ME coefficient of 63 Oe cm/kV.

For FM/PMN-PT (001) heterostructures, *E*-induced butterfly-like magnetic behavior is assumed to be related to 71/180° ferroelectric domain switching of PMN-PT substrate. While the *E*-induced loop-like behavior is considered to be caused by the screening of interfacial charge, magnon-driven ME coupling, or 109° ferroelastic domain switching of PMN-PT. In general, the effect of screening of interfacial charge and magnon-driven ME coupling isn't dominant for sample with thicker FM layer (*i.e.*, more than 100 nm thick). Butterfly-like and loop-like behavior in this work is believed to be resulted from 71°/180° ferroelectric domain switching and 109° ferroelastic domain switching in PMN-PT, respectively.

To confirm the effect of external electric field on ferroelectric and ferroelastic domain structures in PMN-PT substrate, we conducted in-situ PFM measurement for PMN-PT substrate under +6 V and -6 V, as illustrated in figure 5. This kind of measurement can detect both in-plane and out-of-plane phase images of ferroelectrics simultaneously. Figures 5(a), (d) and (g) are references which reflect topography of PMN-PT and simultaneously verify each phase image is from the same area. 109°, 71°, and 180° domain structures (marked with different symbols) are shown in figure 5(c) when there is no voltage applied (original state). After applying +6 V, see figures 5(d), (e) and (f), domains are switched significantly, indicating that electric field can lead to domain switching. To some extent 71°/180° domains are switched back to their original state when -6 V is applied. While there is obvious difference between the original state and the one that is applied -6 V for 109° domain, as shown in figure 5(i). For out-of-plane phase images, 71°/180° domains coexist in the original state (figure 5(b)). +6 V and -6 V can switch domains to 180° (figure 5(e)) and 71° (figure 5(h)) single domain states, respectively. The related evolution of polarization vectors in PMN-PT under different voltages has been reported before, revealing 71°, 180° and 109° domains switching (13,37).

To further confirm the effect of external electric field on magnetic properties of Ni films, *E*-tuning of stripe domain in Ni films was investigated with MFM. Only out-of-plane magnetic domain can be detected in this work. Figure 6 shows evolution of stripe domain with electric field of 0, 3, 10 and 0' kV/cm for Ni film with thickness of 180 nm. Here, 0 and 0' denote the states of sample before applying and after removing electric field, respectively. With the increase of electric

field, some domains are broken, and nearly all of the domains disappear at 10 kV/cm. Finally, the domains appear again at 0' kV/cm, while some of them align along different directions relative to the state at 0 kV/cm. Enlarged MFM images showing stripe domain evolution at consecutive electric fields are illustrated in figure 7(a). Average phase of each MFM image and its variation with electric field are summarized in figure 7(b). It demonstrates a linear relationship between average phase and electric field. Average phase value returns to its original one after removing electric field, which reveals E-tuning of out-of-plane stripe domain is volatile process. This process is possibly related to ferroelectric domain switching in PMN-PT, *i.e.*, 71°/180° ferroelectric domain switching. Similar analyses for other samples with different thicknesses of Ni films are shown in figures S5, S6 and S7. The change of average phase value (ΔP) for all of the Ni films between 0 kV/cm and 10 kV/cm is shown in figure 8. Clearly, thicker films show less E-induced ΔP . 180 nm thick Ni film reaches the highest ΔP of around 28 milli-degrees (m°).

Variation of lattice constants of PMN-PT and Ni film were investigated using XRD under electric field, as shown in figures 9 and S8. Obviously, 10 kV/cm can give rise to left shift of both PMN-PT and Ni film diffraction peaks, leading to the increase of out-of-plane lattice constant (c). E-tuning of c is calculated based on the formula $\Delta c/c$, where Δc is the difference before applying electric field and after applying 10 kV/cm. The values of $\Delta c/c$ for PMN-PT and Ni are 0.15% and 0.1%, respectively. After removing electric field, the diffraction peaks move to right but do not return to original position. Moreover, the diffraction intensity is lower than the situation before applying electric field, implying that the process of E-tuning magnetic properties of Ni/PMN-PT heterostructures is not totally volatile. We've already known volatile behavior (butterfly-like behavior) of Ni film induced by electric field is caused by 71°/180° domain switching, whereas nonvolatile behavior (loop-like behavior) is related to 109° domain switching in current work. Hence, 71°/180° and 109° domain switching coexist in PMN-PT substrate under electric field, which is in consistent with the results shown in figure 5. On the other hand, Ni is negative magnetostriction materials [38], in-plane compressive strain would enhance the in-plane magnetization as well as align the spin along the film plane^[39], see figure 10. Therefore, stripe domain disappears as electric field increased.

In E-tuning FMR measurement, two phenomena of H_r vs E (or H_{me} vs E) are illustrated when magnetic field is applied along edge and diagonal, which could also be attributed to Ni film strain status and magnetic anisotropy of Ni films. Loop-like and butterfly-like H_r vs E (or H_{me} vs E) behavior is induced by interfacial strain between film and substrate that is directly related to E-tuning of ferroelectric and ferroleastic domain switching in PMN-PT substrate [17-19]. In current work, in-plane magnetic easy axis is along diagonal while hard axis is along edge for all of the Ni films, as shown in figures 2 and S2, indicating that the E-tuning effect could also be anisotropic. Furthermore, as mentioned above, the strained part of Ni films plays an important role in determination of magnetic properties when the film is not thick enough. As magnetic field is applied along diagonal, 71°/180° ferroelectric domain and 109° ferroelastic domain are co-dominant in controlling FMR field for thinner Ni films with thicknesses of 180 nm and 240 nm, while 109° ferroelastic domain dominates the tuning of $H_{\rm r}$ for thicker Ni films with thicknesses of 330 nm and 510 nm. Therefore, both loop-like and butterfly-like behavior is observed in figures 3(b) and (d) as well as figures S3(b) and S3(d), nevertheless only loop-like behavior is revealed in figures 4(b) and (d) as well as figures S4(b) and S4(d). Hence, both magnetic anisotropy of Ni films and film strain status can also give rise to anisotropic magnetic response of Ni films.

Above analyses can also be understood from the characterization of *E*-tuning magnetic stripe domain. With the increase of electric field, stripe domain disappears gradually, as seen in figures 6 and 7, unveiling the transformation of magnetic moment from out-of-plane to in-plane direction. The PMN-PT substrates used in this work are the same, implying that all of them have the same ability of tuning magnetic properties. Since *E*-tuning stripe domain is volatile process and is directly related to ferroelectric domain switching, less out-of-plane magnetic moment is mediated for thicker Ni film means less contribution is from 71°/180° ferroelectric domain switching. Consequently, more contribution is from 109° ferroelastic domain switching, which results in loop-like behavior, as shown in figures 3 and 4.

Conclusions

In summary, E-tuning of H_r was conducted in Ni/PMN-PT heterostructures with Ni film

thicknesses of 180 nm, 240 nm, 330 nm and 510 nm. Butterfly-like $H_{\rm r}$ vs E (or $H_{\rm me}$ vs E) curves are shown when magnetic field is applied along edge, while loop-like $H_{\rm r}$ vs E (or $H_{\rm me}$ vs E) curves can be seen as magnetic field applied along diagonal. These findings are related to 71°/180° ferroelectric and 109° ferroelastic domain switching in PMN-PT, film strain status, and magnetic anisotropy in Ni films. This work manifests the feasibility of tailoring loop-like and butterfly-like magnetic behavior via electric field.

Acknowledgements

The authors would like to thank Furong Qiu and Jiahui Yang of Bruker BBIO, Shanghai, for the help of electric-field tuning of FMR measurements. This work was supported by the National Natural Science Foundation of China (Grants No. 51372074, No. 11574073, No. 51571152, No. 11774270, and No. 11974104). The research at Oakland University was supported by grants from the National Science Foundation, United States (DMR-1808892 and ECCS-1923732).

References

- [1] N. A. Spaldin and R. Ramesh, Advances in magnetoelectric multiferroics. Nat. Mater. 18(3): 203-212 (2019)
- [2] N. X. Sun and G. Srinivasan, Voltage Control of Magnetism in Multiferroic Heterostructures and Devices. Spin 02(03): 1240004 (2012)
- [3] M. Liu, O. Obi, J. Lou, S. Stoute, Z. Cai, K. Ziemer and N. X. Sun, Strong magnetoelectric coupling in ferrite/ferroelectric multiferroic heterostructures derived by low temperature spin-spray deposition. J. Phys. D: Appl. Phys. 42(4): 045007 (2009)
- [4] J. Lou, M. Liu, D. Reed, Y. Ren and N. X. Sun, Giant Electric Field Tuning of Magnetism in Novel Multiferroic FeGaB/Lead Zinc Niobate-Lead Titanate (PZN-PT) Heterostructures. Adv. Mater. 21(46): 4711-4715 (2009)
- [5] M. Liu, O. Obi, Z. Cai, J. Lou, G. Yang, K. S. Ziemer and N. X. Sun, Electrical tuning of magnetism in Fe₃O₄/PZN–PT multiferroic heterostructures derived by reactive magnetron sputtering. J. Appl. Phys. 107(7): 073916 (2010)
- [6] Y. Guo, H. Luo, K. Chen, H. Xu, X. Zhang and Z. Yin, Effect of composition and poling field

- on the properties and ferroelectric phase-stability of Pb(Mg _{1/3}Nb_{2/3})O₃–PbTiO₃ crystals. J. Appl. Phys. 92(10): 6134 (2002)
- [7] J.-B. Li, G. Rao, G. Liu, J. Chen, L. Lu, X. Jing, S. Li and J. Liang, Structural transition in unpoled (1–x)PMN–xPT ceramics near the morphotropic boundary. J. Alloy. Compd. 425(1-2): 373-378 (2006)
- [8] P. Zhou, C. Yang, J. Y. Li, X. L. Liu, Z. H. Mei, A. Ye, K. Liang, Z. J. Ma, Y. J. Qi, X. F. Yang and T. J. Zhang, Giant magnetoelectric coefficient of Pb(Zr_{0.52}Ti_{0.48})O₃/La_{0.67}Sr_{0.33}MnO₃ thin film grown on 0.7Pb(Mg_{1/3}Nb_{2/3})O₃–0.3PbTiO₃ single crystal assisted by metglas. Appl. Phys. Express 10(2): 023201 (2017)
- [9] L. Yang, Y. Zhao, S. Zhang, P. Li, Y. Gao, Y. Yang, H. Huang, P. Miao, Y. Liu, A. Chen, C. W. Nan and C. Gao, Bipolar loop-like non-volatile strain in the (001)-oriented Pb(Mg_{1/3}Nb_{2/3})O₃-PbTiO₃ single crystals. Sci. Rep. 4: 4591 (2014)
- [10] Q. Wan, C. Chen and Y. P. Shen, Electromechanical coupling properties of [001], [011] and [111] poled Pb(Mg_{1/3}Nb_{2/3})O₃-0.32PbTiO₃ single crystals. J. Mater. Sci. 41(10): 2993-3000 (2006) [11] Y. Ba, Y. Liu, P. Li, L. Wu, J. Unguris, D. T. Pierce, D. Yang, C. Feng, Y. Zhang, H. Wu, D. Li, Y. Chang, J. Zhang, X. Han, J. Cai, C. W. Nan and Y. Zhao, Spatially Resolved Electric-Field Manipulation of Magnetism for CoFeB Mesoscopic Discs on Ferroelectrics. Adv. Funct. Mater. 1706448 (2018)
- [12] P. Li, Y. Zhao, S. Zhang, A. Chen, D. Li, J. Ma, Y. Liu, D. T. Pierce, J. Unguris, H. G. Piao, H. Zhang, M. Zhu, X. Zhang, X. Han, M. Pan and C. W. Nan, Spatially Resolved Ferroelectric Domain-Switching-Controlled Magnetism in Co₄₀Fe₄₀B₂₀/Pb(Mg_{1/3}Nb_{2/3})_{0.7}Ti_{0.3}O₃ Multiferroic Heterostructure. ACS Appl. Mater. Interfaces 9(3): 2642-2649 (2017)
- [13] S. Zhang, Y. G. Zhao, P. S. Li, J. J. Yang, S. Rizwan, J. X. Zhang, J. Seidel, T. L. Qu, Y. J. Yang, Z. L. Luo, Q. He, T. Zou, Q. P. Chen, J. W. Wang, L. F. Yang, Y. Sun, Y. Z. Wu, X. Xiao, X. F. Jin, J. Huang, C. Gao, X. F. Han and R. Ramesh, Electric-Field Control of Nonvolatile Magnetization in Co₄₀Fe₄₀B₂₀/Pb(Mg_{1/3}Nb_{2/3})_{0.7}Ti_{0.3}O₃ Structure at Room Temperature. Phys. Rev. Lett. 108(13) (2012)
- [14] C. Zhou, M. Zhang, C. Feng, M. Xu, S. Wang and C. Jiang, Magnon-driven interfacial magnetoelectric coupling in Co/PMN-PT multiferroic heterostructures. Phys. Chem. Chem. Phys. 21(38): 21438-21444 (2019)

- [15] C. Zhou, L. Shen, M. Liu, C. Gao, C. Jia and C. Jiang, Strong Nonvolatile Magnon-Driven Magnetoelectric Coupling in Single-Crystal Co/[PbMg_{1/3}Nb_{2/3}O₃]_{0.71}[PbTiO₃]_{0.29} Heterostructures. Phys. Rev. Appl. 9(1) (2018)
- [16] Z. Lai, C. Li, Z. Li, X. Liu, Z. Zhou, W. Mi and M. Liu, Electric field-tailored giant transformation of magnetic anisotropy and interfacial spin coupling in epitaxial γ' -Fe₄N/Pb(Mg_{1/3}Nb_{2/3})_{0.7}Ti_{0.3}O₃ (011) multiferroic heterostructures. J. Mater. Chem. C 7(28): 8537-8545 (2019)
- [17] G. Dunzhu, F. F. Liu, Y. P. Wang, C. Zhou and C. J. Jiang, Electric field tuning non-volatile dynamic magnetism in half-metallic alloys Co₂FeAl/Pb(Mg_{1/3}Nb_{2/3})O₃-PbTiO₃ heterostructure. Mater. Res. Express 6(6): 066114 (2019)
- [18] C. M. Cao, S. W. Chen, K. Y. Yang, G. H. Lan, P. P. Li, W.Q. Wang, M. Liu, G. Z. Chai and C. J. Jiang, Reciprocal-space-resolved piezoelectric control of non-volatile magnetism in epitaxial LiFe₅O₈ film on Pb(Mg_{1/3}Nb_{2/3})_{0.7}Ti_{0.3}O₃ substrate. Appl. Phys. Lett. 114, 112402 (2019)
- [19] C. Zhou, L. Shen, M. Liu, C. Gao, C. Jia, C. Jiang and D. Xue, Long-Range Nonvolatile Electric Field Effect in Epitaxial Fe/Pb(Mg_{1/3}Nb_{2/3})_{0.7}Ti_{0.3}O₃ Heterostructures. Adv. Funct. Mater. 28(20): 1707027 (2018)
- [20] C. Zhang, F. Wang, C. Dong, C. Gao, C. Jia, C. Jiang and D. Xue, Electric field mediated non-volatile tuning magnetism at the single-crystalline Fe/Pb(Mg_{1/3}Nb_{2/3})_{0.7}Ti_{0.3}O₃ interface. Nanoscale 7(9): 4187-4192 (2015)
- [21] X. Zhao, M. Feng, M. Liu, J. Hua, J. Ma, L. Wu, H. Xu, A. P. Wang and H. B. Li, Electric-field tuning of magnetic anisotropy in the artificial multiferroic Fe₃O₄/PMN–PT heterostructure. Mater. Res. Lett. 6(10): 592-597 (2018)
- [22] X. Xue, Z. Zhou, W. Hou, M. Guan, Z. Hu, and M. Liu, Voltage Control of Magnetism Through Two-Magnon Scattering Effect for Magnetoelectric Microwave Devices. IEEE Transactions on Magnetics:1-4 (2018)
- [23] M. Zhu, Z. Zhou, X. Xue, M. Guan, D. Xian, C. Wang, Z. Hu, Z. D. Jiang, Z. G. Ye, W. Ren and M. Liu, Voltage control of spin wave resonance in La_{0.5}Sr_{0.5}MnO₃/PMN-PT (001) multiferroic heterostructures. Appl. Phys. Lett. 111(10): 102903 (2017)
- [24] M. Zhu, Z. Zhou, B. Peng, S. Zhao, Y. Zhang, G. Niu, W. Ren, Z. G. Ye, Y. Liu and M. Liu, Modulation of Spin Dynamics via Voltage Control of Spin-Lattice Coupling in Multiferroics. Adv.

Funct. Mater: 1605598 (2017)

- [25] J. M. Hu, C. W. Nan and L. Q. Chen, Size-dependent electric voltage controlled magnetic anisotropy in multiferroic heterostructures: Interface-charge and strain comediated magnetoelectric coupling. Phys. Rev. B 83(13) (2011)
- [26] F. L. Wang, C. Zhou, C. Zhang, C. H. Dong, C. C. Yang, C. J. Jiang, C. L. Jia and D. S. Xue, Piezoelectric control of magnetic dynamics in Co/Pb(Mg_{1/3}Nb_{2/3})O₃-PbTiO₃ heterostructure. Appl. Phys. Lett. 105(6): 062407 (2014)
- [27] T. Nan, Z. Zhou, M. Liu, X. Yang, Y. Gao, B. A. Assaf, H. Lin, S. Velu, X. Wang, H. Luo, J. Chen, S. Akhtar, E. Hu, R. Rajiv, K. Krishnan, S. Sreedhar, D. Heiman, B. M. Howe, G. J. Brown and N. X. Sun, Quantification of strain and charge co-mediated magnetoelectric coupling on ultra-thin Permalloy/PMN-PT interface. Sci Rep. 4: 3688 (2014)
- [28] Q. X. Zhu, W. Wang, S. W. Yang, X. M. Li, Y. Wang, H.-U. Habermeier, H. S. Luo, H. L. W. Chan, X. G. Li, and R. K. Zheng, Coaction and competition between the ferroelectric field effect and the strain effect in Pr_{0.5}Ca_{0.5}MnO₃ film/0.67Pb(Mg_{1/3}Nb_{2/3})O₃-0.33PbTiO₃ crystal heterostructures. Appl. Phys. Lett. 101(17):172906 (2012)
- [29] C. Feng, Y. Liu, H. Huang, Z. Zhu, Y. Yang, Y. Ba, S. Yan, J. Cai, Y. Lu, J. Zhang, S. Zhang and Y. Zhao, Unusual Behaviors of Electric-Field Control of Magnetism in Multiferroic Heterostructures via Multifactor Cooperation. ACS Appl. Mater. Interfaces 11(28): 25569-25577 (2019)
- [30] Y. Xiang, K. Liang, S. Keller, M. Guevara, M. Sheng, Z. Yan, P. Zhou, Y. Qi, Z. Ma, Y. Liu, G. Srinivasan, G. Carman, T. Zhang, and C. Lynch, Thickness-dependence of magnetic anisotropy and domain structure in Ni thin films grown on a PMN-PT substrate. Smart Mater. Struct (2020) (doi.org/10.1088/1361-665X/aba53d)
- [31] P. Dhanapal, T. Zhang, B. M. Wang, H. L. Yang, H. C. Xuan, C. Bi, W. G. Wang and R. W. Li, Reversibly controlled magnetic domains of Co film via electric field driven oxygen migration at nanoscale. Appl. Phys. Lett. 114, 232401 (2019)
- [32] C. Kittel, On the Theory of Ferromagnetic Resonance Absorption. Phys. Rev. 73(2): 155-161 (1948)
- [33] P. Zhou, A. V. Singh, Z. Li, M. A. Popov, Y. Liu, D. A. Filippov, T. Zhang, W. Zhang, P. J. Shah, B. M. Howe, M. E. McConney, G. Srinivasan, M. R. Page and A. Gupta, Magnetoelectric

- Interactions in Composites of Ferrite Films on Lattice-Matched Substrates and Ferroelectrics. Phys. Rev. Appl. 11(5) (2019)
- [34] G. N. Kakazei, P. E. Wigen, K. Yu. Guslienko, V. Novosad, A. N. Slavin, V. O. Golub, N. A. Lesnik, and Y. Otani, Spin-wave spectra of perpendicularly magnetized circular submicron dot arrays. Appl. Phys. Lett. 85(3):443-445 (2004)
- [35] B. Noheda, D. E. Cox, G. Shirane, J. Gao, and Z. G. Ye, Phase diagram of the ferroelectric-relaxor (1-x)PbMg_{1/3}Nb_{2/3}O₃-xPbTiO₃. Phys. Rev. B 054104 (2002)
- [36] H. X. Fu and R. E. Cohen, Polarization rotation mechanism for ultrahigh electromechanical response in single-crystal piezoelectrics. Nature 403(6767):281-283 (2000)
- [37] M. Zheng, H. Ni, Y. Qi, W. Huang, J. Zeng and J. Gao, Ferroelastic strain control of multiple nonvolatile resistance tuning in SrRuO₃/PMN-PT(111) multiferroic heterostructures. Appl. Phys. Lett. 110(18): 182403 (2017)
- [38] R. R. Birss and E. W. Lee, The saturation magnetostriction constants of nickel within the temperature range-196 to 365 C. Proceedings of the Physical Society 76(4):502-506 (1960)
- [39] R. Zhang, M. Liu, L. Lu, S. B. Mi and H. Wang, Strain-tunable magnetic properties of epitaxial lithium ferrite thin film on MgAl₂O₄ substrates. J. Mater. Chem. C 3(21): 5598-5602 (2015)

Figure Captions

- Figure 1. (a) XRD θ -2 θ pattern, (b) XRD ϕ -scan performed about the (110) crystallographic plane, (c) MFM image of 180 nm (001)-oriented Ni film grown on PMN-PT substrate
- Fgure 2. Angular dependent of FMR field (H_r) for Ni/PMN-PT heterostructures, where dots and lines are experimental data and corresponding fits, respectively. The Ni film thicknesses are 180 nm (a) and 510 nm (b)
- Figure 3. H_r vs E along edge (0°) (a) and diagonal (45°) (b), and H_{me} vs E along edge (0°) (c) and diagonal (45°) (d) for Ni/PMN-PT heterostructure with Ni of 180 nm
- Figure 4. H_r vs E along edge (0°) (a) and diagonal (45°) (b), and H_{me} vs E along edge (0°) (c) and diagonal (45°) (d) for Ni/PMN-PT heterostructure with Ni of 510 nm
- Figure 5. Evolution of in-plane and out-of-plane domains in PMN-PT under electric field of +6 V

and -6 V. (a), (d) and (g) are topographies, (b), (e) and (h) are out-of-plane phase images, (c), (f) and (i) are in-plane phase images

Figure 6. Stripe domain evolution of 180 nm thick Ni film under electric field of 0, 3, 10, and 0' kV/cm

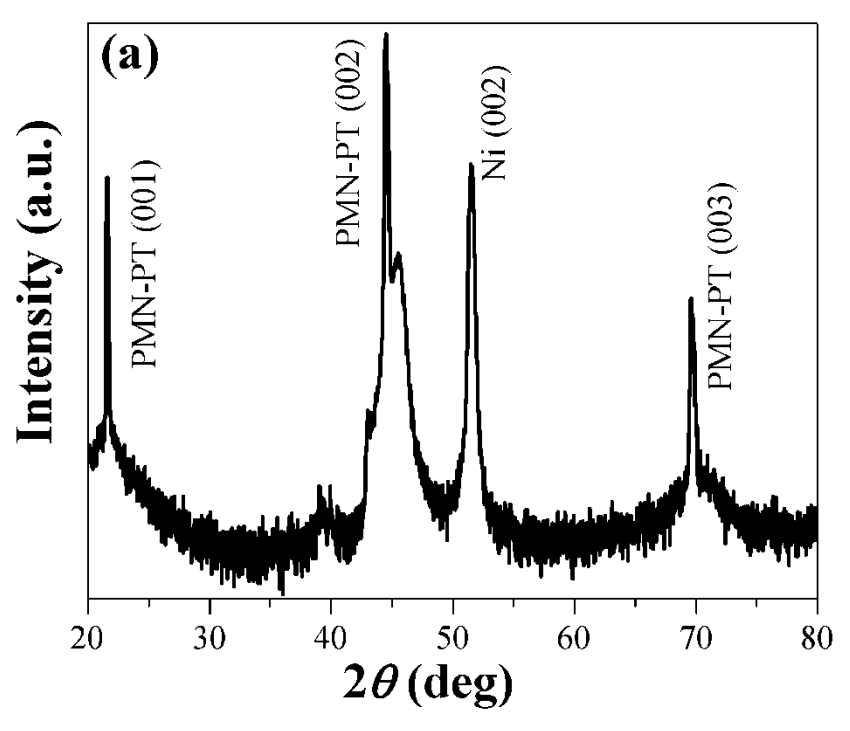
Figure 7. (a) Summary of stripe domain evolution of 180 nm thick Ni film under various electric field values. (b) Electric field dependent of average phase (unit of milli-degree) of stripe domain.

Figure 8.Thickness dependent of average phase change (ΔP), where ΔP defined as the difference of average phase between 0 and 10 kV/cm

Figure 9. (a) XRD (002) peak shift of PMN-PT substrate and (b) XRD (002) peak shift of Ni film under electric field of 0, 10 and 0' kV/cm.

Figure 10. Sketch of response of stripe domain under electric field for Ni/PMN-PT heterostructure. The arrow stands for spin orientation, cross and dot denote magnetization orientation of stripe domain

Table I. Fit values of M_{eff} and H_4 , as well as calculated H_{m} for Ni films with different thickness under no electric field



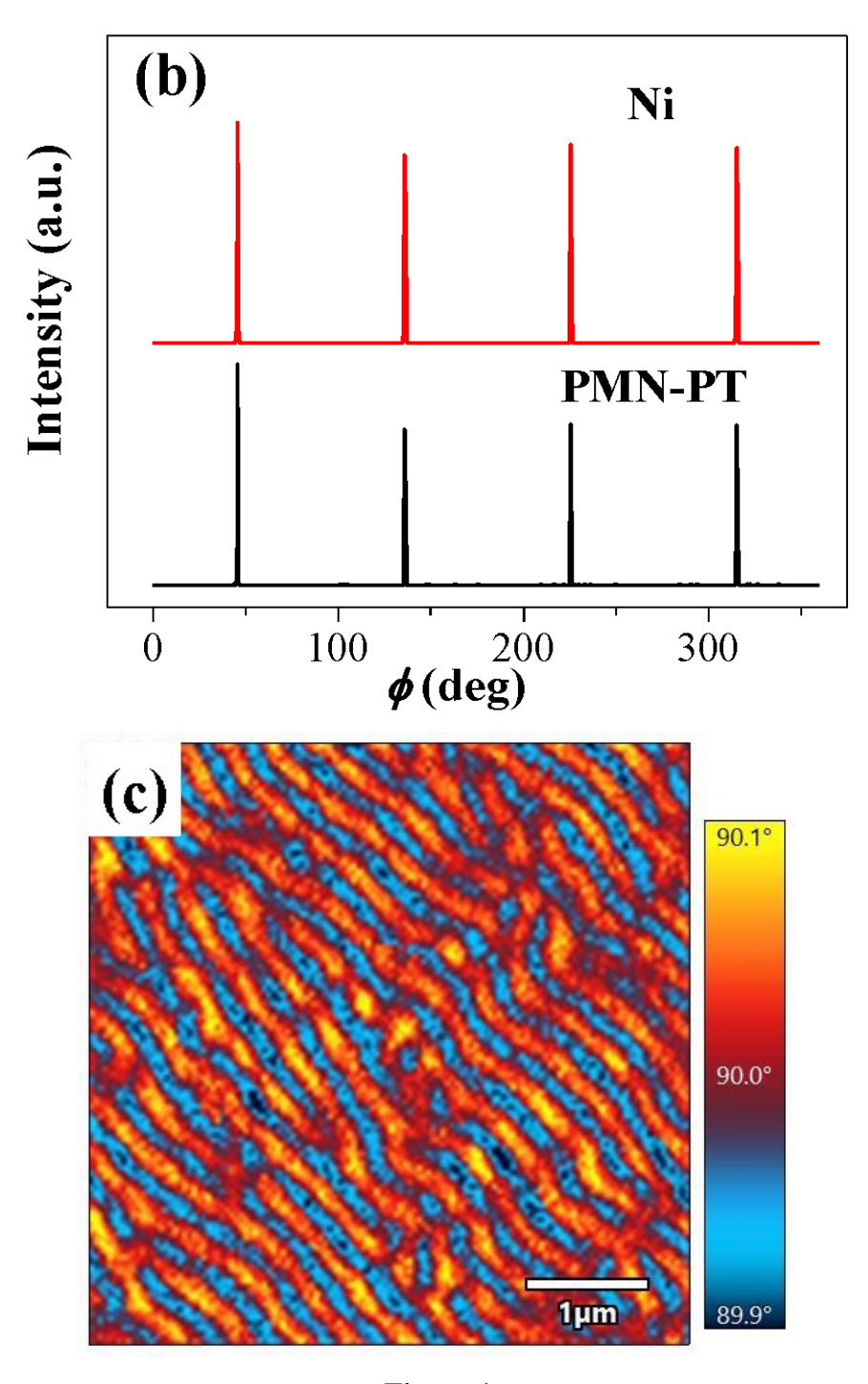


Figure 1

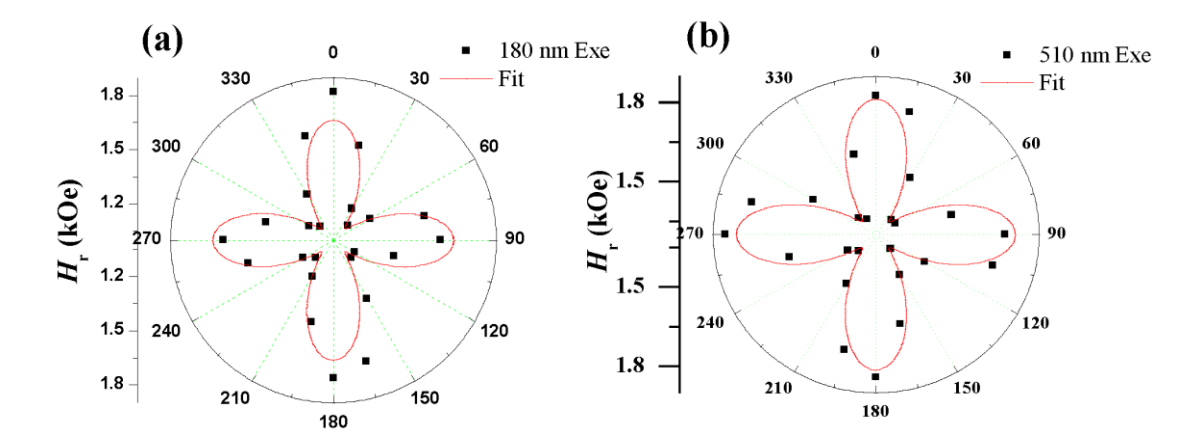
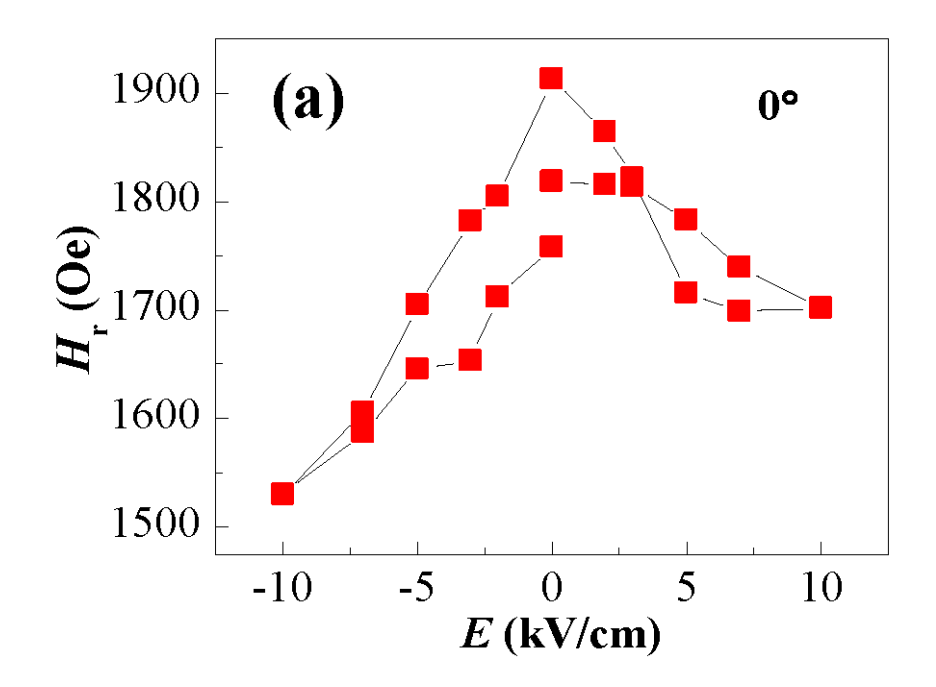
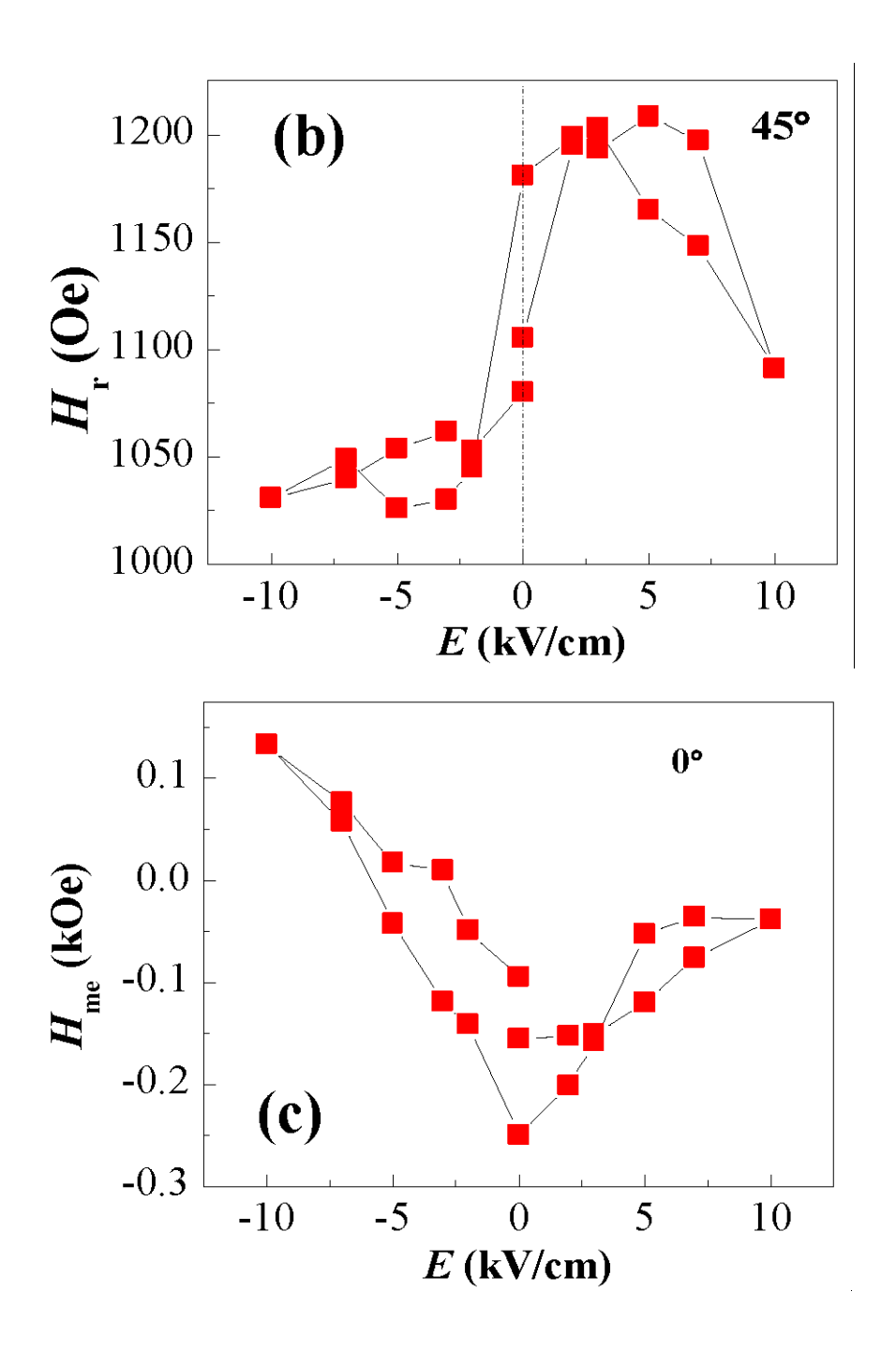
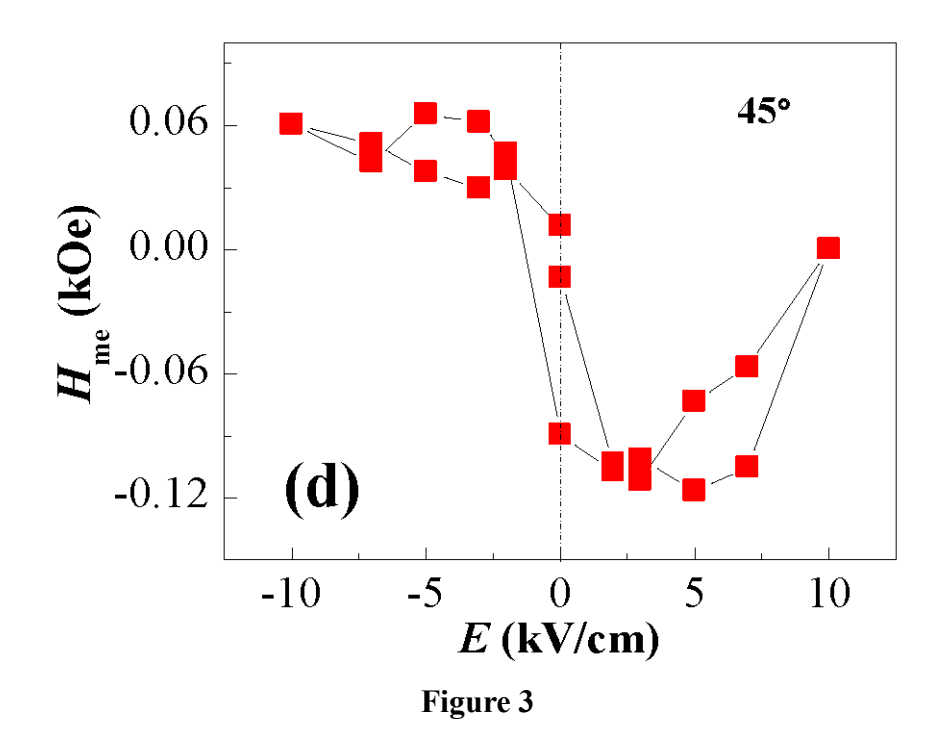
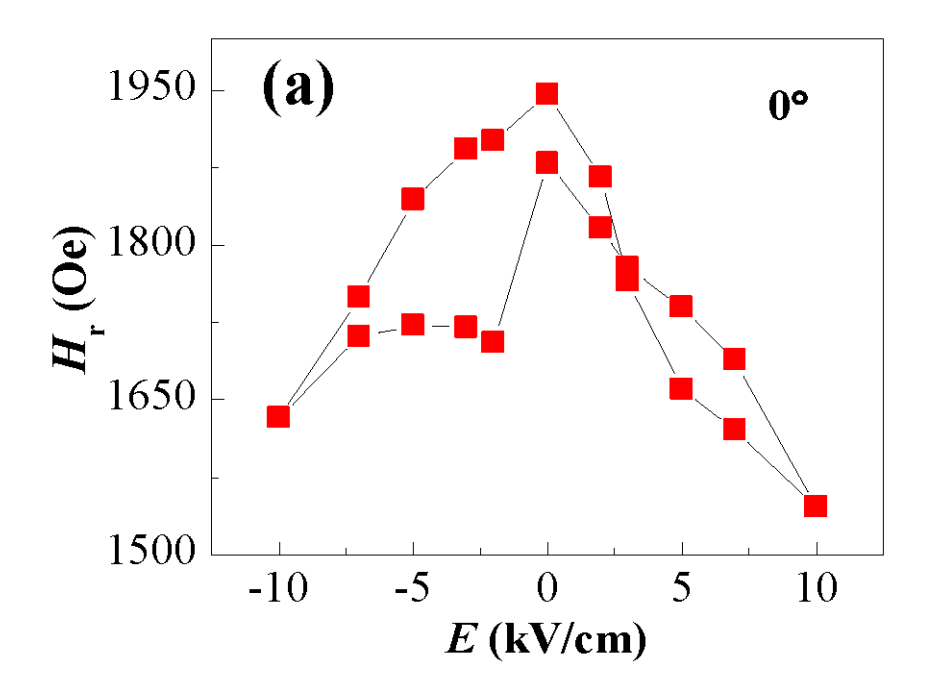


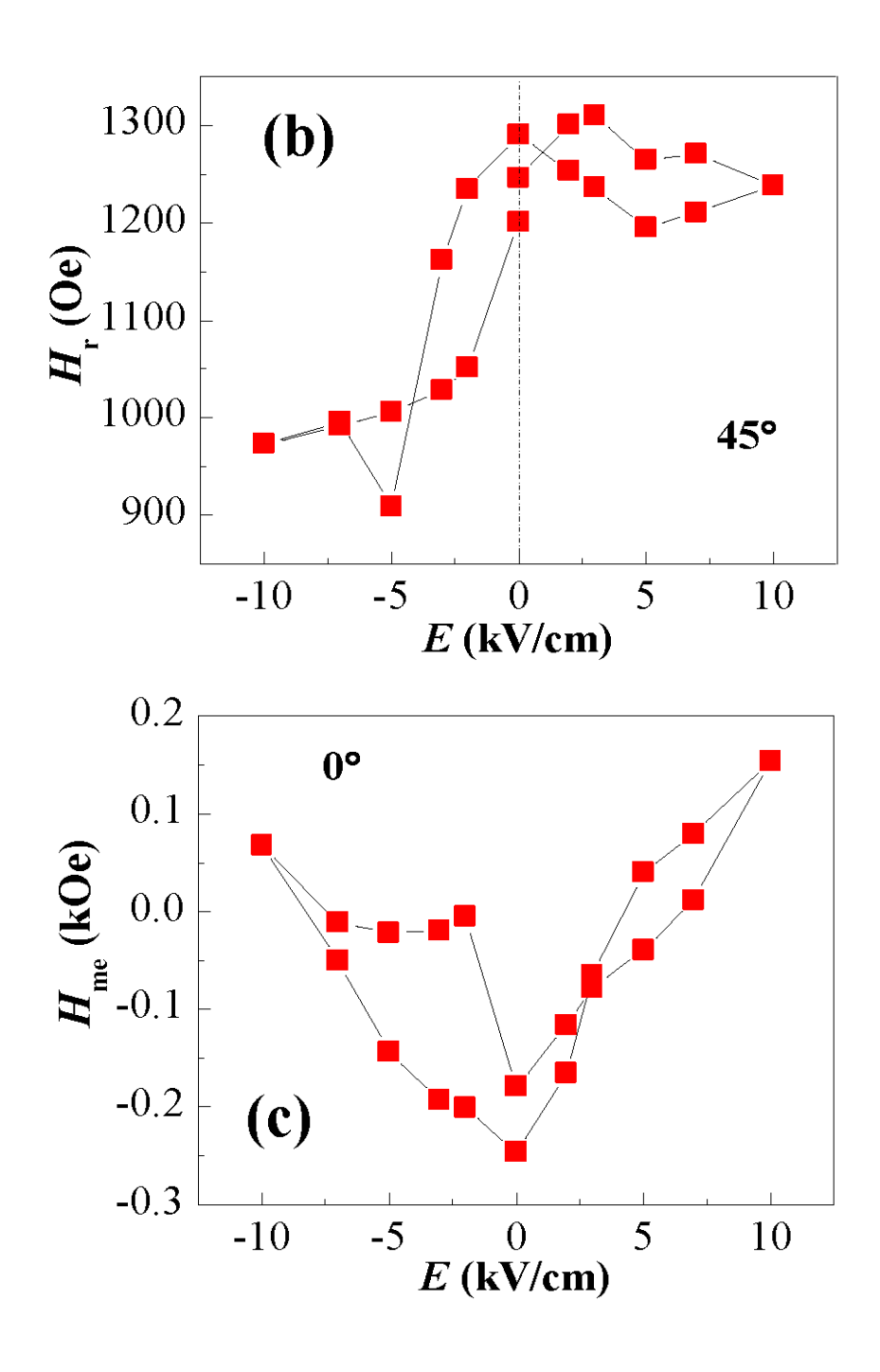
Figure 2

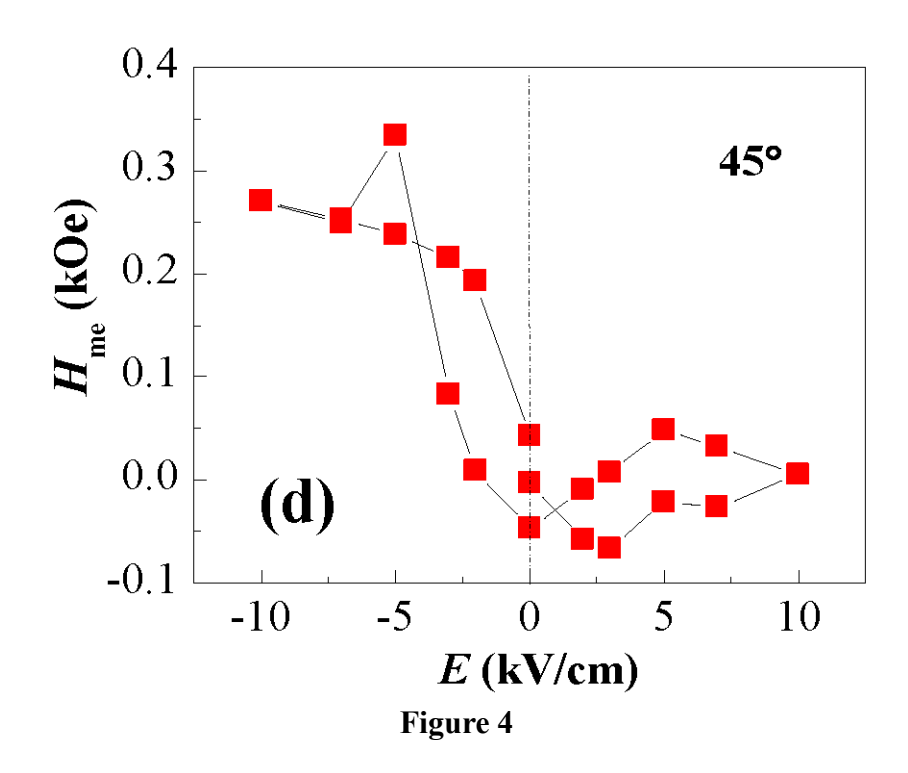












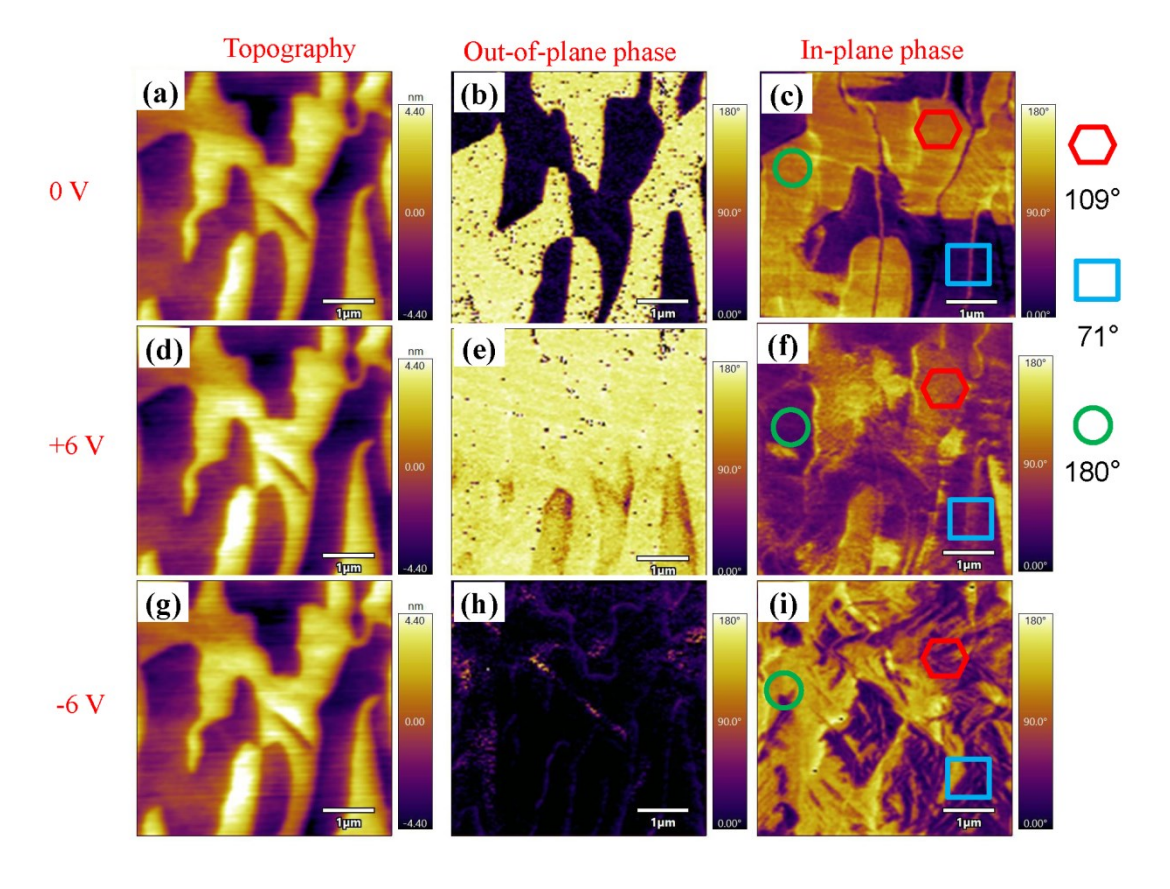


Figure 5

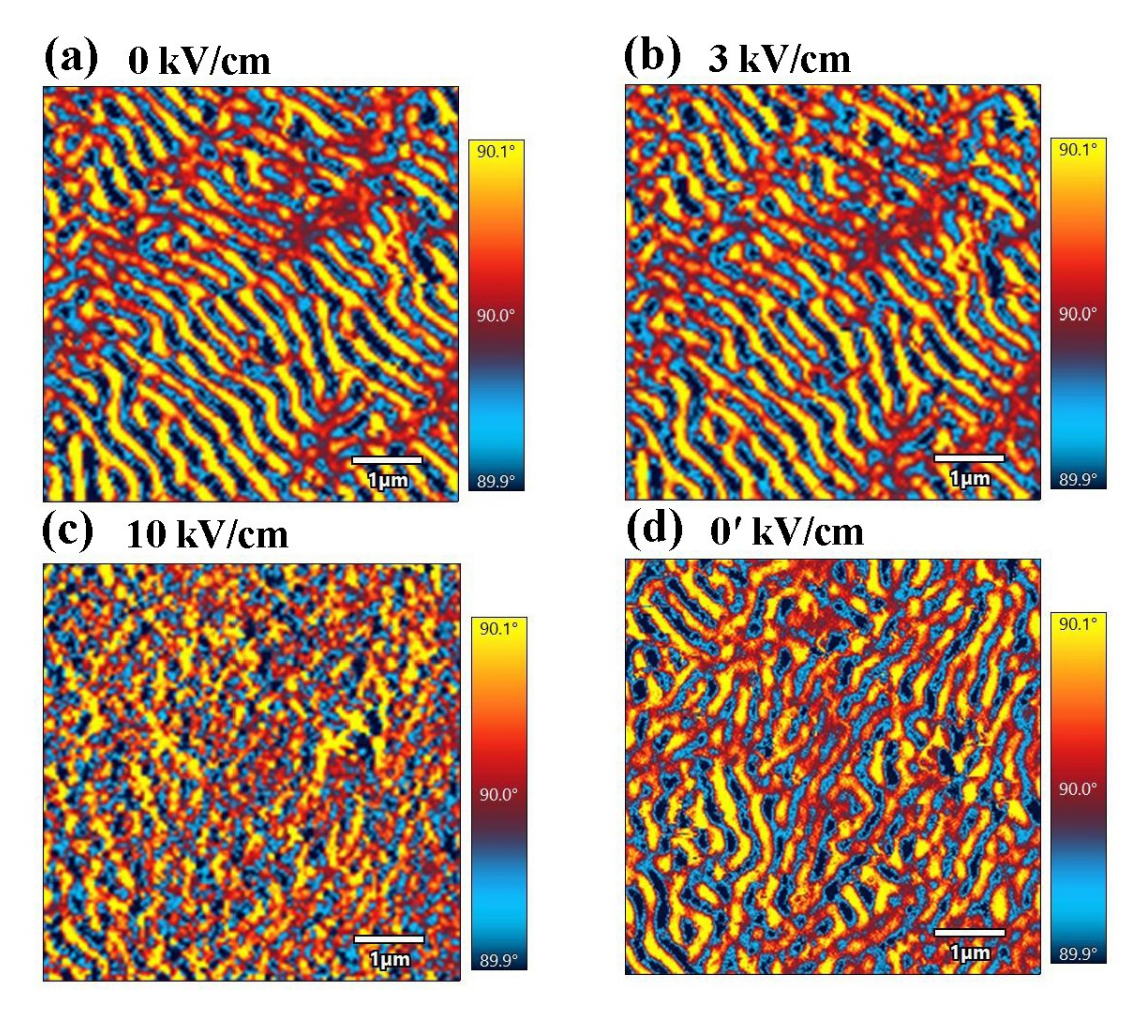


Figure 6

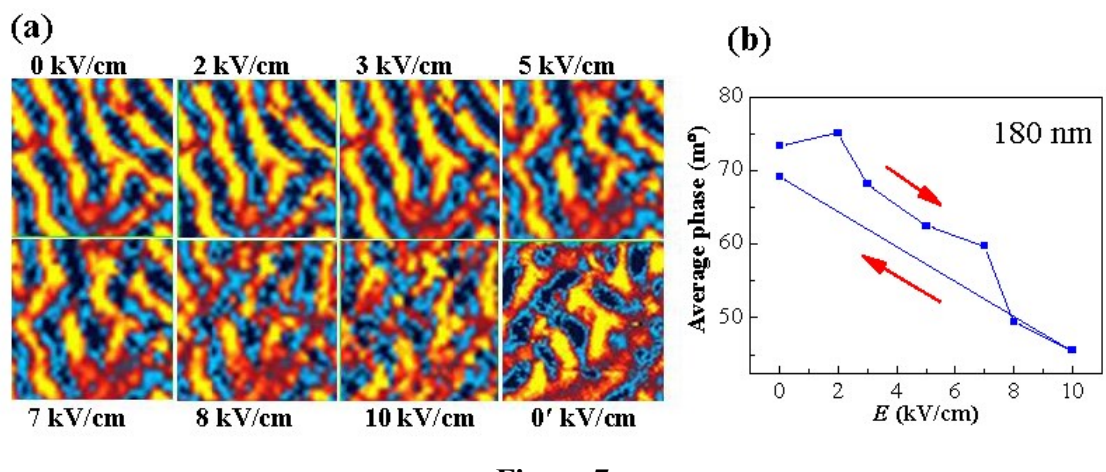


Figure 7

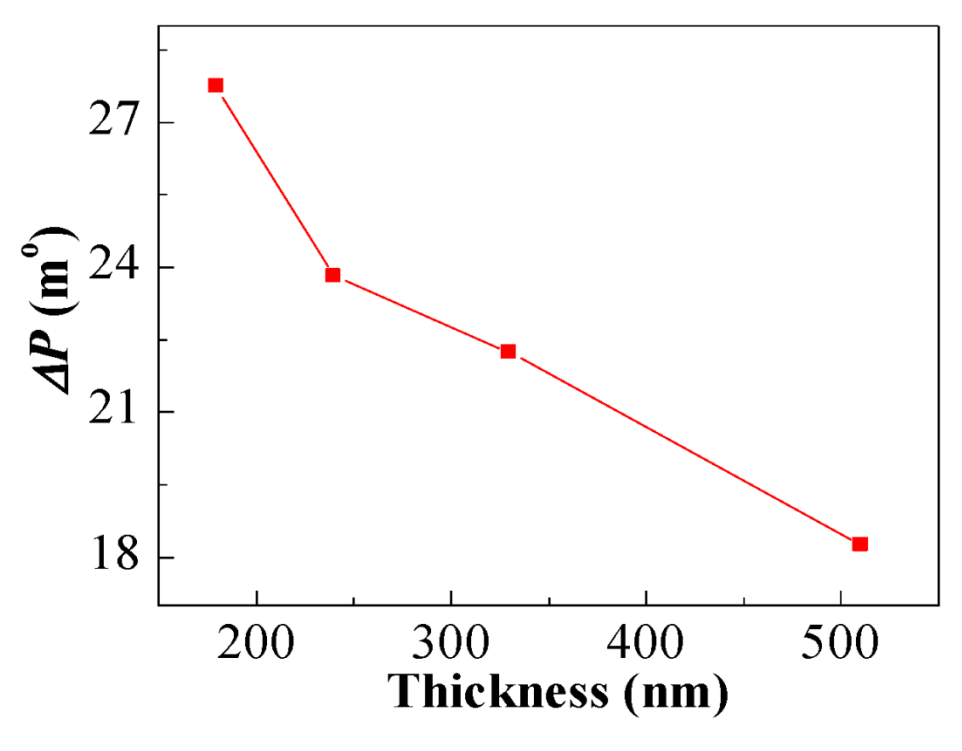
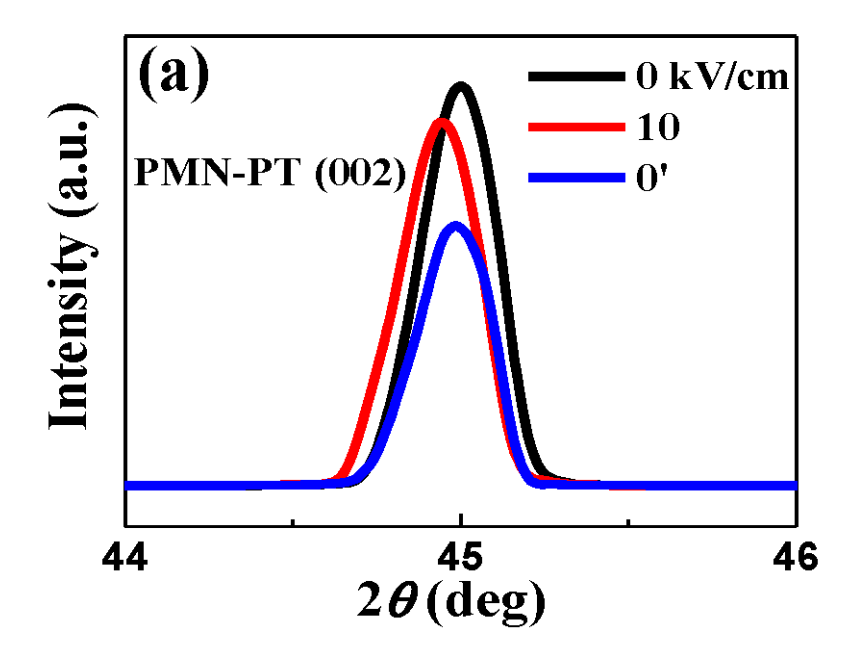
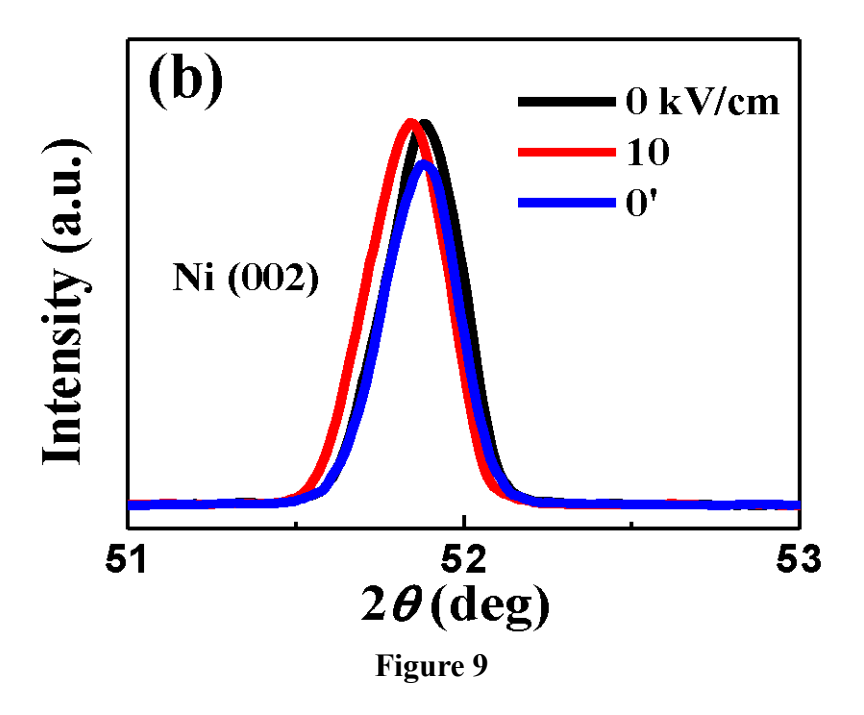


Figure 8





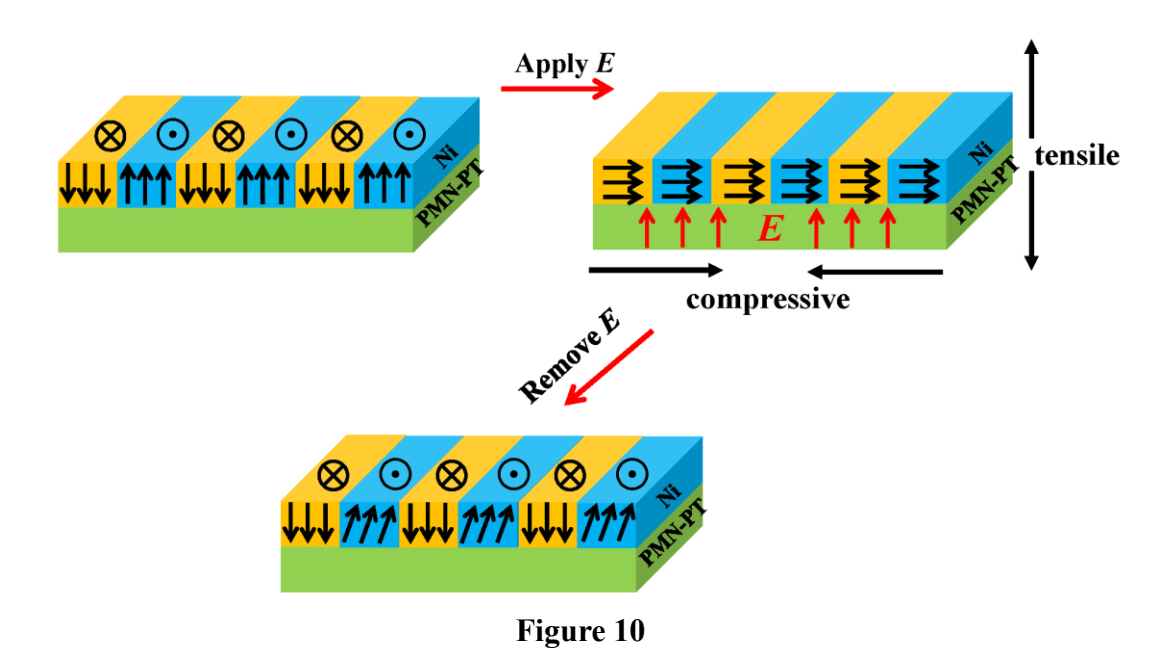


Table I

Thickness (nm)	$M_{\rm eff}$ (kOe)	H_4 (kOe)	H _m (kOe)
180	0.513	-0.323	6.77
240	0.454	-0.303	6.008
330	0.480	-0.284	6.316
510	0.411	-0.259	5.424